THE JOURNAL OF PHYSICAL CHEMISTRY Letters

Letter

Cite This: J. Phys. Chem. Lett. 2018, 9, 678–682

pubs.acs.org/JPCL

Unravelling the Role of an Aqueous Environment on the Electronic Structure and Ionization of Phenol Using Photoelectron Spectroscopy

Jamie W. Riley,[†] Bingxing Wang,[†] Joanne L. Woodhouse, Mariana Assmann, Graham A. Worth, and Helen H. Fielding*

Department of Chemistry, University College London, 20 Gordon Street, London, WC1H 0AJ, United Kingdom

Supporting Information

ABSTRACT: Water is the predominant medium for chemistry and biology, yet its role in determining how molecules respond to ultraviolet light is not well understood at the molecular level. Here, we combine gas-phase and liquid-microjet photoelectron spectroscopy to investigate how an aqueous environment influences the electronic structure and relaxation dynamics of phenol, a ubiquitous motif in many biologically relevant chromophores. The vertical ionization energies of electronically excited states are important quantities that govern the rates of charge-transfer reactions, and, in phenol, the vertical ionization energy of the first electronically excited state is found to be lowered by around 0.8 eV in aqueous solution. The initial relaxation dynamics following photoexcitation with ultraviolet light appear to be remarkably similar in the gas-phase and aqueous solution; however, in aqueous solution, we find evidence to suggest that solvated electrons are formed on an ultrafast time scale following photoexcitation just above the conical intersection between the first two excited electronic states.

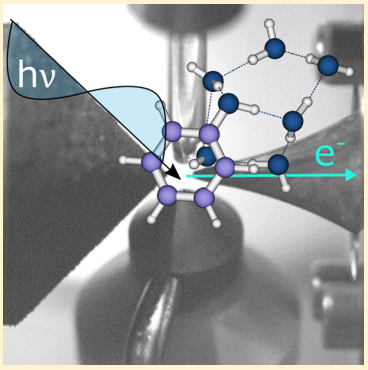

Much of our detailed understanding of the intrinsic electronic relaxation dynamics of photoexcited molecules has come from gas-phase experiments and calculations involving isolated molecules, free from interactions with solvent or protein environments. However, electronically excited states can be very sensitive to their microenvironment, and the extent to which dynamical insights obtained from gas-phase studies can be used to inform our understanding of the dynamics in chemically and biologically relevant environments is a subject of considerable discussion.[1] While it has been shown that the initial relaxation dynamics in weakly interacting solvents may be very similar to those in the gas-phase,[2] this is not necessarily the case for polar solvents such as water, the most important medium in chemistry and biology. Experimentally, the most direct way of probing the electronic structure of a molecule is through the measurement of electron binding energies using photoelectron spectroscopy (PES); however, there are very few PES studies of organic molecules in aqueous solution.[3−7] Here, we employ multiphoton UV PES, both in a molecular beam[8] and a liquid-microjet,[9] to compare the electronic structure and photoionization of phenol in the gas-phase and in an aqueous environment.

Phenol is ubiquitous as a molecular motif in large biologically relevant chromophores; important examples include the amino acid tyrosine, which plays a prominent role in the catalysis of a wide range of enzymes that includes photosystem II, and the chromophore of green fluorescent protein, the most widely used fluorescent probe for *in vivo* monitoring of biological and biochemical processes. There has been a great deal of interest in the interplay between the "optically bright" $^1\pi\pi^*$ states of phenol and the "optically dark" $^1\pi\sigma^*$ states.[10−12] Although the $^1\pi\pi^*$ states are bound in all coordinates, the $^1\pi\sigma^*$ states are dissociative along the O−H coordinate and have been shown to provide efficient electronic relaxation pathways to conical intersections (CIs) with the electronic ground state and thus play an important role in the photostability of chromophores containing the phenol motif.

Phenol absorbs UV radiation around 270 nm (4.6 eV) and 205 nm (6.0 eV) in the gas-phase and in aqueous solution (Figure 1). These bands arise from transitions from the electronic ground state (S_0) to the two lowest lying $^1\pi\pi^*$ states, whose vertical excitation energies (VEEs) are barely perturbed from their gas-phase values by the addition of an aqueous environment. The dissociative $1^1\pi\sigma^*$ state lies between the $1^1\pi\pi^*$ and $2^1\pi\pi^*$ states and, in the gas-phase, has been found to have CIs with the $1^1\pi\pi^*$ state, at $R_{O-H} \sim 1.2$ Å and energy around 5 eV above the S_0 minimum, and with S_0, at $R_{O-H} \sim 2.1$ Å and energy around 4.5 eV above the S_0 minimum.[13,14]

Gas-phase studies of phenol have revealed that O−H bond fission occurs following UV photoexcitation both above and below the $1^1\pi\pi^*/1^1\pi\sigma^*$ CI. Photoexcitation above the $1^1\pi\pi^*/1^1\pi\sigma^*$ CI allows the dissociative $1^1\pi\sigma^*$ potential energy surface to be accessed directly and results in rapid O−H bond fission, on a femtosecond time scale.[15] Photoexcitation below the $1^1\pi\pi^*/1^1\pi\sigma^*$ CI results in O−H bond fission on a nanosecond

Received: December 14, 2017
Accepted: January 22, 2018
Published: January 22, 2018

DOI: 10.1021/acs.jpclett.7b03310
J. Phys. Chem. Lett. 2018, 9, 678–682

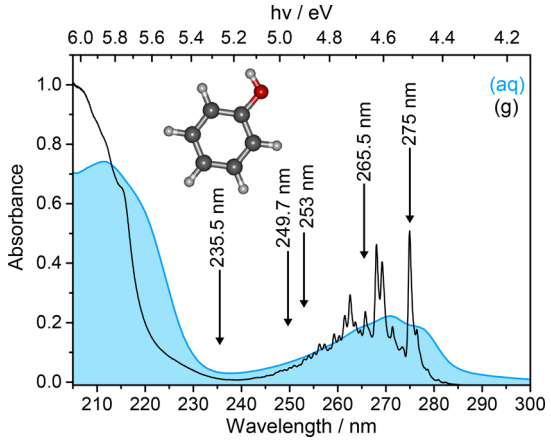

Figure 1. UV absorption spectra of phenol in the gas-phase (black) and in aqueous solution (blue). Vertical arrows indicate the wavelengths employed in our 1 + 1 UV PES measurements. Inset: ground-state minimum energy geometry structure of phenol calculated using the MP2/aug-cc-pVDZ method.

time scale that arises from tunnelling through the barrier under the CI to the dissociative $1^1\pi\sigma^*$ potential energy surface.[10−12] Solution-phase transient absorption studies have shown that in weakly interacting solvents, such as hexane, the initial bond fission process and time scales are very similar to those in the gas-phase.[16] In aqueous solution, solvated electrons have been observed following photoexcitation both above and below the $1^1\pi\pi^*/1^1\pi\sigma^*$ CI (at 200 and 266 nm), on time scales of 200 fs and 2 ns respectively, and attributed to autoionization from excited electronic states to the solvent continuum.[17]

We have employed one-color multiphoton (1 + 1) UV PES to measure and compare the electronic structure and photoionization of phenol in aqueous solution, using a new liquid-microjet photoelectron spectrometer, with analogous measurements in the gas-phase, using our molecular-beam photoelectron spectrometer (Supporting Information). Measuring the electron kinetic energy (eKE) distribution of photoelectrons emitted following photoionization allows us to determine the electron binding energy of the molecular orbital from which the electron is ionized, with respect to the electronic state of the cation that is left behind. The propensity for conserving vibrational energy during photoionization, at least in rigid molecules that do not undergo large amplitude motions, also allows us to use the Franck−Condon distribution of photoelectron eKEs to identify resonant and nonresonant 1 + 1 ionization processes. In Figure 2 we present 1 + 1 UV PES plotted as a function of eKE and as a function of one-photon electron binding energy, eBE = $h\nu$ − eKE, and for 235.5 nm also as a function of two-photon binding energy, eBE = $2h\nu$ − eKE, where $h\nu$ is the photon energy.

It is instructive to begin with a discussion of the gas-phase PES. The 275 nm (4.51 eV) 1 + 1 PES has a sharp peak at 0.51 eV eKE, which, since 275 nm is resonant with the electronic origin of the $1^1\pi\pi^*$-S_0 transition, corresponds to a D_0-$1^1\pi\pi^*$ adiabatic ionization energy (AIE) of 4.0 eV; this is consistent with the literature value for the D_0-S_0 AIE (8.508 eV).[18] Built on the D_0-$1^1\pi\pi^*$ origin is a broad peak centered around 0.25 eV eKE, which corresponds to a D_0-$1^1\pi\pi^*$ vertical ionization energy (VIE) of 4.3 eV. The VIE − AIE difference (~0.3 eV) is the vibrational energy left in D_0 following photoionization from the $1^1\pi\pi^*$ state, consistent with earlier observations.[19]

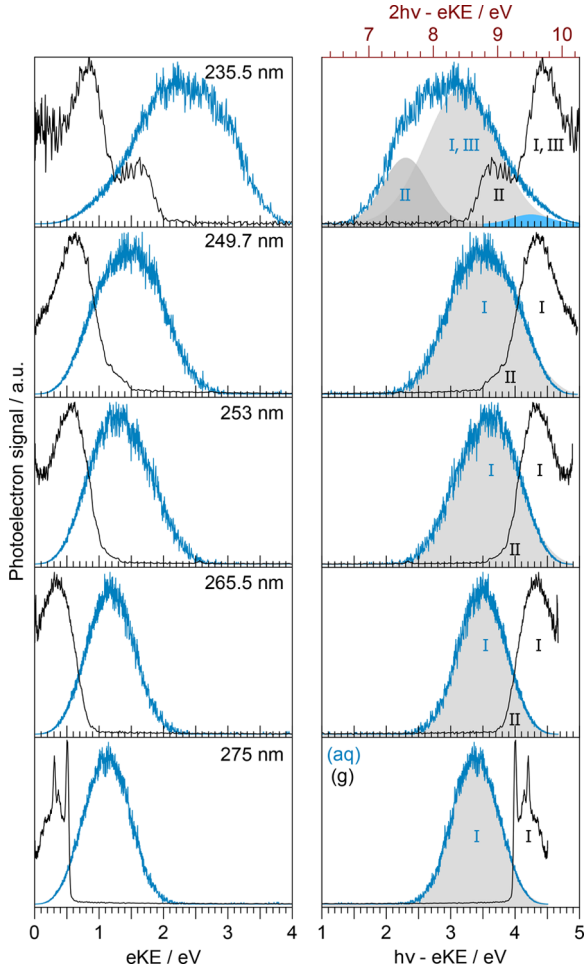

Figure 2. 1 + 1 UV PES of phenol in the gas-phase (black) and in aqueous solution (blue) recorded following photoexcitation at 275 nm (4.51 eV), 265.5 nm (4.67 eV), 253 nm (4.90 eV), 249.7 nm (4.97 eV) and 235.5 nm (5.26 eV), plotted as a function of eKE (left) and one-photon eBE (right). The additional scale marked on the top horizontal axis of the 235.5 nm PES (red) represents the two-photon eBE for this photon energy. Intensities of the individual spectra have been normalized to their maxima. Gray Gaussians represent D_0-$1^1\pi\pi^*$ (I), D_0-S_0 (II), and D_1-S_0 (III) ionization processes (I and III overlap in the 235.5 nm PES and are represented by just one Gaussian), and the blue Gaussian has been assigned to $e^-(aq) \rightarrow e^-(g)$.

The peak centered around 4.3 eV eBE, corresponding to D_0-$1^1\pi\pi^*$ vertical ionization, appears in all the PES (labeled I in Figure 2); however, photoexcitation at 235.5 nm is not expected to populate the $1^1\pi\pi^*$ state directly (Figure 1). Thus, the observation of D_0-$1^1\pi\pi^*$ ionization suggests that following photoexcitation above the $1^1\pi\pi^*/1^1\pi\sigma^*$ CI, the $1^1\pi\pi^*$ state is populated by rapid internal conversion (IC) from the $1^1\pi\sigma^*$ state, which is populated directly, on the time scale of the measurement (~300 fs), and that the lifetime of the $1^1\pi\pi^*$ state is longer than this.

For λ < 275 nm, a small peak appears on the low eBE edge of the D_0-$1^1\pi\pi^*$ feature (labeled II in Figure 2); it remains at constant two-photon eBE (Supporting Information) and is therefore attributed to 1 + 1 nonresonant ionization from S_0. The D_0-S_0 VIE can be read directly from the two-photon eBE scale on the top horizontal axis of the 235.5 nm 1 + 1 PES (~8.8 eV).

DOI: 10.1021/acs.jpclett.7b03310
J. Phys. Chem. Lett. 2018, 9, 678−682

Calculations of photoionization cross sections for 1 + 1 nonresonant ionization from S_0 and 1 + 1 resonant ionization via the $1^1\pi\pi^*$ state of phenol to the D_0 and D_1 states of the phenol cation (Figure 3) show that the $1^1\pi\pi^*$ state ionizes

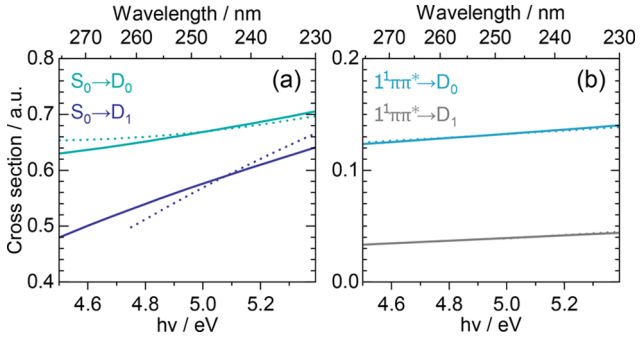

Figure 3. (a) One-photon photoionization cross sections from the S_0 state of phenol to the D_0 and D_1 states of the phenol cation plotted as a function of photon energy for an equivalent two-photon (1 + 1 nonresonant) ionization process. (b) One-photon photoionization cross sections for ionization from the $1^1\pi\pi^*$ state of phenol to the D_0 and D_1 states of the phenol cation plotted as a function of photon energy. Calculations were performed for isolated molecules in the gas-phase (dashed lines) and clusters of phenol $+6H_2O$ (solid lines). Dyson orbital norms were calculated using the EOM-IPEE-CCSD/aug-cc-pVDZ method (Supporting Information).

predominantly to D_0 and that the S_0 state ionizes to both D_0 and D_1, but with a higher probability of ionizing to D_0 at the photon energies employed in these experiments. The D_1-S_0 AIE is approximately 9.36 eV;[20] coincidentally, at 235.5 nm, this ionization process produces electrons with very similar eKEs to those generated by 1 + 1 resonant D_0-$1^1\pi\pi^*$ ionization, which explains why the 235.5 nm PES is dominated by only two peaks and why the peak at higher eBE, which has contributions from D_0-$1^1\pi\pi^*$ ionization (labeled I in Figure 2) and D_1-S_0 (labeled III in Figure 2), is more intense than the peak at lower eBE corresponding to D_0-S_0 ionization (labeled II in Figure 2).

We now focus on the aqueous-phase PES. The spectra recorded in aqueous solution are all shifted to higher eKEs (lower eBEs) by around 0.8 eV compared to those in the gas-phase. For wavelengths in the range 275−249.7 nm, the resonant 1 + 1 PES can be fit to a single Gaussian with maxima centered around 3.5 ± 0.1 eV eBE, corresponding to the D_0-$1^1\pi\pi^*$ VIE. The peak positions vary slightly as a result of changes in the Franck−Condon overlap between the $1^1\pi\pi^*$ and D_0 states. The widths of the peaks depend on the reorganization energy of phenol and the aqueous solution. Inelastic electron scattering in the liquid-jet is also likely to influence the measured eBEs and peak widths.[21] It will be interesting to model the PES and unravel the contribution from electron scattering, in future work, as this would allow the determination of the reorganization energy which, together with the VIE, would enable calculation of the one-electron standard reduction potential, an important parameter in determining charge transport rates.

At 235.5 nm, where the UV absorption cross-section is low (Figure 1), direct ionization from S_0 to D_0 and D_1 competes with resonant 1 + 1 ionization. At this photon energy, we find the PES can be fit with Gaussians centered at 2.9 ± 0.1 eV and 2.0 ± 0.1 eV eKE, which correspond to 7.6 ± 0.1 eV and 8.5 ± 0.1 eV two-photon eBEs; these are equivalent to the D_0-S_0 and D_1-S_0 VIEs, respectively. As with gas-phase phenol, coincidentally, the D_1-S_0 and D_0-$1^1\pi\pi^*$ ionization processes generate electrons with similar eKEs, which explains why the spectrum is dominated by only two peaks and why the area of the Gaussian centered at higher eBE is much larger than the area of the Gaussian centered at lower eBE. Our measured D_0-S_0 and D_1-S_0 VIEs are in good agreement with those measured using XUV synchrotron radiation at BESSY II (7.8 ± 0.1 eV and 8.5 ± 0.1 eV) and those determined using the EOM-IP-CCSD/EFP method (7.9 eV and 8.6 eV);[3] the variations between the experimental values may arise from the streaming potential which, although often assumed to be insignificant, was accounted for in our measurements (Supporting Information). As with the gas-phase PES, it is noteworthy that there is evidence of D_0-$1^1\pi\pi^*$ ionization in the 235.5 nm PES, since the $1^1\pi\pi^*$ state is not expected to be populated directly at this wavelength (Figure 1). This suggests that, similar to the gas-phase, the $1^1\pi\sigma^*$ state is excited directly, and population flows rapidly to the $1^1\pi\sigma^*/1^1\pi\pi^*$ CI, where some undergoes IC to the $1^1\pi\pi^*$ state, on the time scale of the measurement in aqueous solution (∼150 fs), and some continues on the dissociative $1^1\pi\sigma^*$ surface.

There is a tail on the high eBE edge of the 235.5 nm spectrum that cannot be described without the addition of a third Gaussian centered at 4.2 ± 0.1 eV eBE (one-photon). Energetically, this can be attributed to D_1-$1^1\pi\pi^*$ ionization (we would expect the difference between the VIEs from $1^1\pi\pi^*$ to D_0 and D_1 to be similar to the difference between the VIEs from S_0 to D_0 and D_1, which is 0.9 eV) or the PES of the solvated electron, $e^-(aq) \rightarrow e^-(g)$.[21,22] It seems unlikely that D_1-$1^1\pi\pi^*$ ionization would be observed only in the 235.5 nm spectrum, which has a significant contribution from direct ionization from S_0 to D_0 and D_1, and not in the PES at longer wavelengths, which are dominated by resonant 1 + 1 ionization via the $1^1\pi\pi^*$ state; therefore, we believe the most likely explanation for the feature around 4.2 eV eBE is the formation of solvated electrons on the time scale of the measurement (∼150 fs).

The formation of solvated electrons on an ultrafast time scale following photoexcitation of organic molecules with acidic hydrogen atoms is not without precedent.[23] Solvated electrons have been observed to be formed within 200 fs following 260 nm photoexcitation of indole in aqueous solution[24] and 200 nm photoexcitation of the second absorption band of phenol in aqueous solution.[17] The mechanism for the formation of solvated electrons following 200 nm photoexcitation of phenol was proposed to be autoionization from electronically excited states to form $PhOH^+(aq) + e^-(aq)$. In contrast, following 200 nm photoexcitation of phenol in cyclohexane, $PhO^\bullet$ radicals were formed within 200 fs but solvated electrons were not observed.[25] In our experiment, we observe significant D_0-$1^1\pi\pi^*$ ionization and solvated electrons following photoexitation at 235.5 nm, below the second absorption band. Our observation is consistent with direct population of the $1^1\pi\sigma^*$ state and rapid relaxation to the $1^1\pi\pi^*/1^1\pi\sigma^*$ CI, followed by some population undergoing IC to $1^1\pi\pi^*$ and some undergoing O−H dissociation to form $PhO^\bullet$+H, followed by proton-coupled electron transfer, $H(aq) + H_2O \rightarrow H_3O^+(aq) + e^-(aq)$, on the time scale of our experiment (∼150 fs).

Although we cannot completely rule out the possibility that autoionisation competes with relaxation on the $1^1\pi\sigma^*$ potential energy surface, PCET is consistent with calculations of hydrogen atom transfer to the solvent shell in phenol-water

DOI: 10.1021/acs.jpclett.7b03310
J. Phys. Chem. Lett. 2018, 9, 678−682

clusters following relaxation on the $1^1\pi\sigma^*$ state.[13] The value of the eBE (4.2 eV) merits discussion as it is similar to accurate measurements of the maximum eBE in PES of fully solvated electrons using photon energies of 5.2 and 5.4 eV (~4.0 eV eBE).[21,22] Although solvation times are typically considered to be longer than the time scale of our measurement (~150 fs), the OH bond of phenol is already part of a network of hydrogen-bonded water molecules, so it is possible that the electron is formed in an environment close to its fully solvated form. Future time-resolved PES measurements should be able to shed light on the time scales for the formation of fully equilibrated solvated electrons following relaxation on a $1^1\pi\sigma^*$ potential energy surface, which are expected to be different to those for solvation of electrons formed by autoionization[17] or from charge-transfer to solvent (CTTS) states of anions.[26,27]

In summary, we have shown that comparing analogous 1 + 1 UV PES measurements of chromophores in aqueous solution and the gas-phase promises to be a powerful method for unravelling the role of an aqueous environment on the VIEs of excited electronic states of chromophores and their relaxation dynamics following UV photoexcitation. VIEs of excited states in aqueous solution are difficult to measure using other methods but play an important role in determining the kinetics of charge transfer processes. In phenol, we have found that an aqueous environment lowers the VIE of the first excited electronic state by around 0.8 eV. Moreover, although the initial relaxation dynamics appear similar in the gas-phase and in aqueous solution, we have found evidence to suggest that solvated electrons are formed within ~150 fs following photoexcitation just above the conical intersection between the $1^1\pi\pi^*$ and $1^1\pi\sigma^*$ states of phenol in aqueous solution.

■ ASSOCIATED CONTENT

Supporting Information

The Supporting Information is available free of charge on the ACS Publications website at DOI: 10.1021/acs.jpclett.7b03310.

Experimental methods; photoelectron spectra plotted as a function of two-photon eBE; fits to 235.5 nm photoelectron spectra of aqueous phenol; velocity-map images; computational methods; calculated structures of phenol + $n$$H_2O$; calculated VIEs and VEEs; ionization cross sections of phenol + $n$$H_2O$ (PDF)

■ AUTHOR INFORMATION

Corresponding Author

*E-mail: h.h.fielding@ucl.ac.uk.

ORCID

Helen H. Fielding: 0000-0003-1572-0070

Author Contributions

†These authors contributed equally to this work

Notes

The authors declare no competing financial interest.

■ ACKNOWLEDGMENTS

The authors thank the EPSRC (EP/L005646/1 and EP/L005697/2) and the Diamond Light Source (STU0157) for funding, Dr. Michael Parkes and Dr. Yu Zhang for technical assistance, and Dr. Tom Oliver (Bristol) for useful discussions.

■ REFERENCES

(1) Ashfold, M. N. R. Photoinitiated Quantum Molecular Dynamics: Concluding Remarks. *Faraday Discuss.* **2013**, *163*, 545−551.

(2) Ashfold, M. N. R.; Murdock, D.; Oliver, T. A. A. Molecular Photofragmentation Dynamics in the Gas and Condensed Phases. *Annu. Rev. Phys. Chem.* **2017**, *68*, 63−82.

(3) Ghosh, D.; Roy, A.; Seidel, R.; Winter, B.; Bradforth, S.; Krylov, A. I. First-Principle Protocol for Calculating Ionization Energies and Redox Potentials of Solvated Molecules and Ions: Theory and Application to Aqueous Phenol and Phenolate. *J. Phys. Chem. B* **2012**, *116*, 7269−7280.

(4) Palivec, V.; Pluhařová, E.; Unger, I.; Winter, B.; Jungwirth, P. DNA Lesion Can Facilitate Base Ionization: Vertical Ionization Energies of Aqueous 8-Oxoguanine and its Nucleoside and Nucleotide. *J. Phys. Chem. B* **2014**, *118*, 13833−13837.

(5) Buchner, F.; Nakayama, A.; Yamazaki, S.; Ritze, H.-H.; Lübcke, A. Excited-State Relaxation of Hydrated Thymine and Thymidine Measured by Liquid-Jet Photoelectron Spectroscopy: Experiment and Simulation. *J. Am. Chem. Soc.* **2015**, *137*, 2931−2938.

(6) Tentscher, P. R.; Seidel, R.; Winter, B.; Guerard, J. J.; Arey, J. S. Exploring the Aqueous Vertical Ionization of Organic Molecules by Molecular Simulation and Liquid Microjet Photoelectron Spectroscopy. *J. Phys. Chem. B* **2015**, *119*, 238−256.

(7) Schroeder, C. A.; Pluhařová, E.; Seidel, R.; Schroeder, W. P.; Faubel, M.; Slavíček, P.; Winter, B.; Jungwirth, P.; Bradforth, S. E. Oxidation Half-Reaction of Aqueous Nucleosides and Nucleotides *via* Photoelectron Spectroscopy Augmented by *ab initio* Calculations. *J. Am. Chem. Soc.* **2015**, *137*, 201−209.

(8) Fielding, H. H.; Worth, G. A. Using Time-Resolved Photoelectron Spectroscopy to Unravel the Electronic Relaxation Dynamics of Photoexcited Molecules. *Chem. Soc. Rev.* **2018**, *47*, 309−321.

(9) Seidel, R.; Winter, B.; Bradforth, S. E. Valence Electronic Structure of Aqueous Solutions: Insights from Photoelectron Spectroscopy. *Annu. Rev. Phys. Chem.* **2016**, *67*, 283−305.

(10) Nix, M. G.; Devine, A. L.; Cronin, B.; Dixon, R. N.; Ashfold, M. N. R. High Resolution Photofragment Translational Spectroscopy Studies of the Near Ultraviolet Photolysis of Phenol. *J. Chem. Phys.* **2006**, *125*, 133318.

(11) Roberts, G. M.; Chatterley, A. S.; Young, J. D.; Stavros, V. G. Direct Observation of Hydrogen Tunneling Dynamics in Photoexcited Phenol. *J. Phys. Chem. Lett.* **2012**, *3*, 348−352.

(12) Livingstone, R. A.; Thompson, J. O. F.; Iljina, M.; Donaldson, R. J.; Sussman, B. J.; Paterson, M. J.; Townsend, D. Time-Resolved Photoelectron Imaging of Excited State Relaxation Dynamics in Phenol, Catechol, Resorcinol and Hydroquinone. *J. Chem. Phys.* **2012**, *137*, 184304.

(13) Sobolewski, A. L.; Domcke, W. Photoinduced Electron and Proton Transfer in Phenol and its Clusters with Water and Ammonia. *J. Phys. Chem. A* **2001**, *105*, 9275−9283.

(14) Dixon, R. N.; Oliver, T. A. A.; Ashfold, M. N. R. Tunnelling under a Conical Intersection: Application to the Product Vibrational State Distributions in the UV Photodissociation of Phenols. *J. Chem. Phys.* **2011**, *134*, 194303.

(15) Iqbal, A.; Cheung, M. S. Y.; Nix, M. G. D.; Stavros, V. G. Phenol-D5: Statistical vs Nonstatistical Decay. *J. Phys. Chem. A* **2009**, *113*, 8157−8163.

(16) Harris, S. J.; Murdock, D.; Zhang, Y.; Oliver, T. A. A.; Grubb, M. P.; Orr-Ewing, A. J.; Greetham, G. M.; Clark, I. P.; Towrie, M.; Bradforth, S. E.; et al. Comparing Molecular Photofragmentation Dynamics in the Gas and Liquid Phases. *Phys. Chem. Chem. Phys.* **2013**, *15*, 6567−6582.

(17) Oliver, T. A. A.; Zhang, Y.; Roy, A.; Ashfold, M. N. R.; Bradforth, S. E. Exploring Autoionization and Photoinduced Proton-Coupled Electron Transfer Pathways of Phenol in Aqueous Solution. *J. Phys. Chem. Lett.* **2015**, *6*, 4159−4164.

(18) Lipert, R. J.; Colson, S. D. Field Dependence of the Pump-Probe Photoionization Threshold. *J. Chem. Phys.* **1990**, *92*, 3240−3241.

DOI: 10.1021/acs.jpclett.7b03310
J. Phys. Chem. Lett. 2018, 9, 678−682

(19) Anderson, S. L.; Goodman, L.; Krogh-Jespersen, K.; Ozkabak, A. G.; Zare, R. N.; Zheng, C.-f. Multiphoton Ionization Photoelectron Spectroscopy of Phenol: Vibrational Frequencies and Harmonic Force Field for the 2B1 Cation. *J. Chem. Phys.* **1985**, *82*, 5329−5339.
(20) Dewar, M. J. S.; Worley, S. D. Photoelectron Spectra of Molecules. I. Ionization Potentials of Some Organic Molecules and Their Interpretation. *J. Chem. Phys.* **1969**, *50*, 654−667.
(21) Luckhaus, D.; Yamamoto, Y.-i.; Suzuki, T.; Signorell, R. Genuine Binding Energy of the Hydrated Electron. *Sci. Adv.* **2017**, *3*, e1603224.
(22) Yamamoto, Y. I.; Karashima, S.; Adachi, S.; Suzuki, T. Wavelength Dependence of UV Photoemission from Solvated Electrons in Bulk Water, Methanol, and Ethanol. *J. Phys. Chem. A* **2016**, *120*, 1153−1159.
(23) Abel, B.; Buck, U.; Sobolewski, A. L.; Domcke, W. On the Nature and Signatures of the Solvated Electron in Water. *Phys. Chem. Chem. Phys.* **2012**, *14*, 22−34.
(24) Peon, J.; Hess, G. C.; Pecourt, J.-M. L.; Yuzawa, T.; Kohler, B. Ultrafast Photoionization Dynamics of Indole in Water. *J. Phys. Chem. A* **1999**, *103*, 2460−2466.
(25) Zhang, Y.; Oliver, T. A. A.; Ashfold, M. N. R.; Bradforth, S. E. Contrasting the Excited State Reaction Pathways of Phenol and *para*-methylthiophenol in the Gas and Liquid Phases. *Faraday Discuss.* **2012**, *157*, 141−163.
(26) Kloepfer, J. A.; Vilchiz, V. H.; Lenchenkov, V. A.; Germaine, A. C.; Bradforth, S. E. The Ejection Distribution of Solvated Electrons Generated by the One-Photon Photodetachment of Aqueous I- and Two-Photon Ionization of the Solvent. *J. Chem. Phys.* **2000**, *113*, 6288−6307.
(27) Elkins, M. H.; Williams, H. L.; Shreve, A. T.; Neumark, D. M. Relaxation Mechanism of the Hydrated Electron. *Science* **2013**, *342*, 1496−1499.

DOI: 10.1021/acs.jpclett.7b03310
J. Phys. Chem. Lett. 2018, 9, 678−682